Renewable Energy 113 (2017) 1311–1319

Contents lists available at ScienceDirect

Renewable Energy

journal homepage: www.elsevier.com/locate/renene

Dynamic simulation of two-tank indirect thermal energy storage system with molten salt

Xiaolei Li [a, b, c, d], Ershu Xu [a, b, c, d, *], Shuang Song [a, b, c, d], Xiangyan Wang [e], Guofeng Yuan [a, b, c, d]

[a] Key Laboratory of Solar Thermal Energy and Photovoltaic System of Chinese Academy of Sciences, Beijing, 100190, China
[b] Institute of Electrical Engineering, Chinese Academy of Sciences, Beijing, 100190, China
[c] Beijing Engineering Research Center of Solar Thermal Power, Beijing, 100190, China
[d] University of Chinese Academy of Sciences, Beijing, 100049, China
[e] China Electric Power Research Institute, Nanjing, Jiangsu, 210003, China

ARTICLE INFO

Article history:
Received 17 January 2017
Received in revised form
28 April 2017
Accepted 4 June 2017
Available online 6 June 2017

Keywords:
Thermal energy storage
Two tank
Simulation

ABSTRACT

Thermal energy storage system, which can effectively store solar energy and make a solar power plant generate electricity in cloudy or rainy weather and nighttime, is a key part of a concentrating solar power plant, which makes solar power technology have unique advantages compared with other renewable energy power technology. Two-tank indirect thermal energy storage system with molten salt is most widely used and has been successfully commercialized in the field of solar power. In this passage, a universal dynamic simulation model of two-tank indirect thermal energy storage system with molten salt used for trough solar power plants based on the lumped parameter method is built, and the dynamic processes of thermal energy storage system charge and discharge, and the changes of heat transfer oil outlet temperature in the oil/salt heat exchanger, molten salt temperature and height in the molten salt tank when heat transfer oil mass flow rate has step disturbances are simulated on the STAR-90 simulation platform. The simulation results show that the model can simulate the charge and discharge dynamic characteristics of two-tank indirect thermal energy storage system with molten salt well, which can be good references for the system design, system control and system debugging.

© 2017 Published by Elsevier Ltd.

1. Introduction

With the extensive use of fossil fuels, global pollution problem is getting more and more serious. The use of renewable energy has been paid more and more attention to by many countries around the world. Solar power technology is one of solar energy utilization technology. Compared with other renewable energy power technology, such as photovoltaic, wind power, solar power technology can realize generating electricity continually in cloudy or rainy weather and nighttime using the thermal energy storage system, which can overcome the intermittent of solar energy and can achieve peak power regulation, making the output power meet the needs of the grid. These advantages described above make solar power technology has similar operability as traditional coal-fired power technology [1]. Moreover, the use of thermal energy storage system also reduces the cost of solar power technology. Some studies have shown that the levelized electricity cost (LEC) of solar power technology can be reduced by about 10% with a thermal storage of 12 h [2].

Until now there are two kinds of thermal energy storage systems operated commercially including two-tank thermal energy storage system with molten salt and steam accumulator. Two-tank thermal energy storage system with molten salt is the most widely used in a lot of concentrating solar power plants. Two-tank thermal energy storage system with molten salt can be divided into two parts, two-tank direct thermal energy storage system with molten salt and two-tank indirect thermal energy storage system with molten salt. The latter is more common, especially in the parabolic trough solar power plant. Two-tank indirect thermal energy storage system with molten salt includes oil/salt heat exchanger and molten salt tanks (hot salt tank and cold salt tank). In the charging process, heat transfer oil flows into the oil/salt heat exchanger after

* Corresponding author. Key Laboratory of Solar Thermal Energy and Photovoltaic System of Chinese Academy of Sciences, Beijing, 100190, China; Institute of Electrical Engineering, Chinese Academy of Sciences, Beijing, 100190, China.
E-mail address: xuershu@mail.iee.ac.cn (E. Xu).

http://dx.doi.org/10.1016/j.renene.2017.06.024
0960-1481/© 2017 Published by Elsevier Ltd.

Nomenclature

A_i	inner area of heat exchanger's tube bundle (m^2)
A_o	outer area of heat exchanger's tube bundle (m^2)
A_{tank}	area of molten salt tank (m^2)
c_p	specific heat capacity (J/(kg·K))
c_{p_oil}	specific heat capacity of heat transfer oil (J/(kg·K))
$c^0_{p\_oil}$	specific heat capacity of heat transfer oil at the previous time step (J/(kg·K))
c_{p_salt}	specific heat capacity of molten salt (J/(kg·K))
$c_{p\_salt\_out}$	specific heat capacity of outlet molten salt (J/(kg·K))
c_{p_tube}	specific heat capacity of heat transfer tubes (J/(kg·K))
d_i	inner diameter of heat transfer tubes (m)
d_o	outer diameter of heat transfer tubes (m)
f	friction factor (−)
h_{oil_in}	specific enthalpy of inlet heat transfer oil (J/kg)
h_{oil_out}	specific enthalpy of outlet heat transfer oil (J/kg)
$h^0_{oil\_out}$	specific enthalpy of outlet heat transfer oil at the previous time step (J/kg)
h_{salt_in}	specific enthalpy of inlet molten salt (J/kg)
h_{salt_out}	specific enthalpy of outlet molten salt (J/kg)
H_{salt}	height of molten salt in the tank (m)
l	heat transfer tube length (m)
m_{oil}	total mass of heat transfer oil at the tube side (kg)
m^0_{oil}	total mass of heat transfer oil at the tube side at the previous time step (kg)
m_{salt}	total mass of molten salt at the shell side (kg)
m_{tube}	total mass of heat exchanger's tube bundle (kg)
$m(t)$	mass of molten salt in the tank (kg)
m_0	initial mass of molten salt in the tank (kg)
Pr_f	Prandtl number of fluid (−)
Pr_w	Prandtl number of fluid based on tube wall temperature as reference temperature (−)
q_{m_oil}	mass flow rate of heat transfer oil (kg/s)
q_{m_salt}	mass flow rate of molten salt (kg/s)
Q_{oil}	heat flow rate between heat transfer oil and tube wall (W)
Q_{salt}	heat flow rate between molten salt and tube wall (W)
Re	Reynolds number (−)
Re_f	Reynolds number of molten salt (−)
R	radius of molten salt tank (m)
T	temperature (K)
T_{oil}	temperature of heat transfer oil (K)
T^0_{oil}	temperature of heat transfer oil at the previous time step (K)
T_{oil_in}	temperature of inlet heat transfer oil (K)
T_{oil_out}	temperature of outlet heat transfer oil (K)
$T^0_{oil\_out}$	temperature of outlet heat transfer oil at the previous time step (K)
T_{tube}	temperature of tube wall (K)
T^0_{tube}	temperature of tube wall at the previous time step (K)
T_{salt}	temperature of molten salt (K)
T_{salt_in}	temperature of inlet molten salt (K)
T_{salt_out}	temperature of outlet molten salt (K)
$T(t)$	temperature of molten salt in the tank (K)
T_{amb}	ambient temperature (K)
T_{ref}	reference temperature (K)
t	time (s)
$u(t)$	specific internal energy of molten salt in the tank (J/kg)
α	heat transfer coefficient at the oil side (J/(m^2·K))
α'	heat transfer coefficient at the molten salt side (J/(m^2·K))
α_{tank}	heat loss coefficient of the tank (J/(m^2·K))
Δt	time step (s)
λ	thermal conductivity (W/(m·K))
μ	dynamic viscosity (Pa·s)
ν	kinematic viscosity (m^2/s)
ρ	density (kg/m^3)
ρ_{salt}	density of molten salt in the tank (kg/m^3)

absorbing heat from the solar field and molten salt is also driven into the oil/salt heat exchanger from cold salt tank by the molten salt pump. Then in the oil/salt heat exchanger, heat transfer oil releases heat to molten salt. Finally, molten salt flows into hot salt tank for heat storage after absorbing heat from heat transfer oil; discharging process is charging process in reverse, molten salt is driven into the oil/salt heat exchanger from hot salt tank by the molten salt pump, releases heat to heat transfer oil, and then flows back to the cold salt tank. Heat transfer oil flows into power block after absorbing heat to finish power cycle. The schematic diagram of charging and discharging processes are shown in Fig. 1.

In this passage, the dynamic simulation model of oil/salt heat exchanger and that of molten salt tanks are built respectively, which constitute the dynamic simulation model of two-tank indirect thermal energy storage system with molten salt together.

The process of heat transfer between heat transfer oil and molten salt is accomplished by oil/salt heat exchanger, which determines the performance of the thermal energy storage system to a large degree, so the heat exchanger is the most important component for the whole system and modeling of the heat exchanger is crucial regarding system dynamic simulations. Currently, the tube-and-shell heat exchanger is most commonly used and there is a lot of literature describing methods of building tube-and-shell heat exchanger dynamic models, which can be divided into two groups: The first one is based on the method of computational fluid dynamics and three-dimension heat exchanger numerical models with high precision are built; the second one is dynamic models of lower spatial resolution than the first one, such as one-dimension heat exchanger models.

Heat exchanger models based on the method of computational fluid dynamics takes detailed heat exchanger structures into consideration, such as baffle shapes and numbers, tubes layout and inlet and outlet nozzles. It can accomplish comprehensive performance evaluation and optimization of heat exchangers. However, this method needs plenty of computation and a high speed computer is absolutely required.

Yang et al. [3] developed 3-D numerical simulations of a rod-baffle shell-and-tube heat exchanger with four different modeling approaches and compared numerical results with experimental results. The whole model based on computational fluid dynamics had highest accuracy but demanded significant computational resources. Lee [4] proposed a modified three-dimensional numerical model for the borehole ground heat exchanger and validated the model by experimental data. The conclusion that a short-time-step model should be used in a long-term dynamic system simulation was reached. Leoni et al. [5] analyzed the shell side flow in a shell and tube heat exchanger using computational fluid dynamics and considered two single-segmental-baffle geometries, with and without baffle clearances. Simulation results showed that baffle clearances reduced temperature peaks along the exchanger and

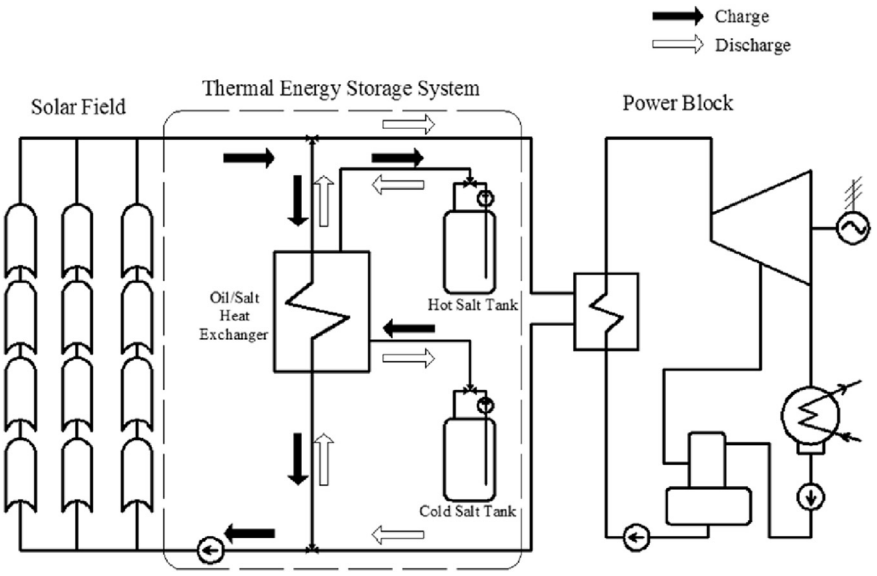

Fig. 1. The schematic diagram of charging and discharging processes.

pressure drop on the baffle window. Fabio De Bellis et al. [6] proposed an innovative immersed particle heat exchanger and optimized the heat exchanger design, such as diameters and angles of inlet and outlet pipes and particle injection mode, using computational fluid dynamics method. Such performance simulations and optimization were accomplished by Ambekar et al. [7], Yehia et al. [8] and Yang et al. [9].

Due to less computational effort, the second modeling method is more simple and flexible and can be used for heat exchanger dynamic simulations that are good references for designing control strategies [10]. Maestre et al. [11] presented a new hybrid two-dimensional model to simulate single U-tube ground heat exchangers. The number of equations were reduced because heat transfer equations were discretized only within the borehole domain and ground temperature nodes were not considered. The model was successfully validated through comparison with a numerical reference model based on computational fluid dynamics. Rees [12] developed an extended two-dimensional borehole heat exchanger model and a novel heat exchanger analogy that iterative procedures can be avoided and numerical stability was unconditional was employed. Model validation was accomplished by comparison with experimental data and by comparing two and three-dimensional model behaviour in the frequency domain. The model was computationally efficient enough for routine analysis and design tasks. One-dimension models including analytical models and numerical models are more common as for this method. One-dimension analytical models applies the Laplace transform to solve partial differential equations. One-dimension numerical models are based on the finite volume method and discretized into certain numbers of control volumes in one-dimension space. As a result, partial differential equations based on mass, momentum and energy balances for the entire model are changed into ordinary differential equations for one control volume. Then ordinary differential equations are transformed into algebraic equation set, which can be solved by numerical algorithms to get final simulation results. For instance, Tse et al. [13] introduced the design of an indirect thermosyphon solar water heating system coupled with a parallel circular tube rings type heat exchanger and the insulated water tank and the heat exchange coil set were modeled. The tank was divided into five layers with equal height along the fluid flow direction and the energy balanced equation of each layer was written. The experimental and simulations results showed good agreements and the accuracy of the entire model was confirmed.

In the field of concentrating solar power, one-dimension numerical modeling method for analyzing tube-and-shell heat exchangers is usually adopted because it is convenient for performance simulations and control strategy design at the whole plant level. Manenti et al. [14] built the dynamic model of Archimede concentrating solar power plant and detailed mathematical models of the economizer and thermal energy storage tanks based on first-principles were presented. The economizer model was discretized into 10 elements and every element was separated into 6 windows. Then one window was considered as one control volume and ordinary differential equations were obtained. The simulation result showed that the dynamic model could be used to evaluate the performance of the concentrating solar power plant. Zaversky et al. [10] applied the cell-method, a specific application of the finite volume method, to model multi-pass shell-and-tube heat exchangers used in active indirect thermal energy storage systems for concentrated solar power. According to different flow conditions, the tube bundle were divided into 2 cross-flow zones and 4 window zones and shell side flow model was separated into 11 control volumes. The governing ordinary differential equations based on mass and energy balances were listed, which were solved by differential-algebraic system solver DASSL. Model validation was accomplished by comparing simulation results to theoretical as well as experimental data available in the literature. And transient response simulation results and suitable degrees of discretization were also discussed. Bonilla et al. [15] presented a preliminary object-oriented dynamic multi-pass shell-and-tube heat exchanger model. The model was built based on the finite volume method and verified against design data. Then dynamic simulation results were compared with experimental data obtained from CIEMAT-PSA molten salt testing facility in steady-state and transient conditions and the performance detriment of the heat exchanger was estimated.

In the present paper, the dynamic model based on the lumped parameter method of the oil/salt heat exchanger used for two-tank indirect thermal energy storage system with molten salt is mainly

described. This kind of dynamic model is more universal than the one-dimension numerical model regardless of specific flow patterns of the fluid in the heat exchanger.

2. Methodology

In this passage, the modeling method of oil/salt heat exchanger is similar to the second modeling methods mentioned above, but the oil side, the wall side and the salt side of the heat exchanger are respectively modeled based on the lumped parameter method instead of the finite volume method, which construct zero-dimension dynamic model of the heat exchanger. Compared with the second modeling method, this method is more universal because specific fluid flow patterns need not be identified once again as for a different heat exchanger and more simple without separating the tube side and the shell side space into control volumes according to fluid flow patterns, such as cross-flow zone and counter-flow zone. The lumped parameter method treats state parameters of the fluid in the tube side and shell side of the heat exchanger as uniform and one typical point is chosen, state parameters of which are lumped parameters in the corresponding space. There are two simple and typical points, which are the middle point representing arithmetic mean values of inlet parameters and outlet parameters and the outlet point respectively. The former reflects fluid mean parameters and the latter reflects fluid parameter variation results in the fluid space. However, there are some problems using the lumped parameter method. When the middle point parameter is chosen as the lumped parameter, the outlet parameter negative deviation will take place during dynamic simulations. For example, when the inlet temperature of the fluid in the tube side or shell side of the heat exchanger increases, the outlet temperature of that will decrease first and then increase, which is not reasonable obviously. When the outlet point parameter is chosen as the lumped parameter, inverse heat transfer will take place for cross-flow heat transfer because the hot fluid outlet temperature may be lower than cold fluid outlet temperature. On the contrary, the model based on finite volume method is reasonable and the more control volumes are, the more precise the model is. But more control volumes means more computation. In this passage, only the mass flow rate is changed during dynamic simulations and no negative deviation will take place, therefore the lumped parameter method that the middle point parameter is chosen as the lumped parameter is used, which is simple and accurate enough.

Then the molten salt tank model is also built based on the lumped parameter method and constitutes the dynamic simulation model of two-tank indirect thermal energy storage system with molten salt together with the oil/salt heat exchanger model. The simulation results show that the model can simulate dynamic processes of the system well and be good references for the system design, system control and system debugging.

2.1. Physical properties of heat transfer oil and molten salt

The variation of heat transfer oil and molten salt physical properties with temperature is considered in this passage since the variation range of heat transfer oil and molten salt physical properties with temperature is large. Therminol-VP1 is used as heat transfer oil and Solar Salt (60% $NaNO_3$ and 40% KNO_3) is used as molten salt. There is literature presenting the physical properties of the two kinds of working fluid, which are listed below:

The physical properties of Therminol-VP1 [16] (12 °C–425 °C, T is in°C):

Density (kg/m^3):

$$\rho = -0.90797 \times T + 0.00078116 \times T^2 - 2.367 \times 10^{-6} \times T^3 + 1083.25 \quad (1)$$

Specific heat capacity (J/(kg·K)):

$$c_p = 2.414 \times T + 5.9591 \times 10^{-3} \times T^2 - 2.9879 \times 10^{-5} \times T^3 + 4.4172 \times 10^{-8} \times T^4 + 1498 \quad (2)$$

Thermal conductivity (W/(m·K)):

$$\lambda = -8.19477 \times 10^{-5} \times T - 1.92257 \times 10^{-7} \times T^2 + 2.5034 \times 10^{-11} \times T^3 - 7.2974 \times 10^{-15} \times T^4 + 0.137743 \quad (3)$$

Kinematic viscosity (m^2/s):

$$\nu = e^{\left(\frac{544.149}{T+114.43} - 2.59578\right)} \times 10^{-6} \quad (4)$$

The physical properties of Solar Salt [17] (270 °C–600 °C, T is in°C):

Density (kg/m^3):

$$\rho = 2090 - 0.636 \times T \quad (5)$$

Specific heat capacity (J/(kg·K)):

$$c_p = 1443 + 0.172 \times T \quad (6)$$

Thermal conductivity (W/(m·K)):

$$\lambda = 0.443 + 1.9 \times 10^{-4} \times T \quad (7)$$

Dynamic viscosity (Pa/s):

$$\mu = \left(22.714 - 0.120 \times T + 2.281 \times 10^{-4} \times T^2 - 1.474 \times 10^{-7} \times T^3\right) \times 10^{-3} \quad (8)$$

2.2. The model of oil/salt heat exchanger

In this passage, tube-and-shell heat exchanger is chosen as the type of oil/salt heat exchanger. Tube side fluid is heat transfer oil and shell side fluid is molten salt. Due to the corrosive effects of molten salt, the material of the parts which are in contact with the molten salt, such as heat transfer tubes and shell cylinder must be anti-corrosive. The material commonly used of the heat exchanger is carbon steel, but in this passage S30403 stainless steel is selected, which has good anti-corrosion. Besides, different materials just lead to different coefficient values, namely specific heat capacities and densities, which will not change the thermal energy storage system model and have little impact on simulation results. Oil/salt heat exchanger parameters are shown in Table 1.

The following assumptions are used when oil/salt heat exchanger is modeled:

Working fluid flow rates remain constant;

Since this passage focuses on the changes of the working fluid temperature and heat transfer process is single-phase heat transfer, working fluid pressure drop is not considered;

Table 1
Oil/salt heat exchanger parameters.

Design parameters	Data
Area of heat transfer (m^2)	3234
Number of shell-side passes (−)	1
Number of tube-side passes (−)	2
Tube outer diameter (m)	0.016
Tube inner diameter (m)	0.012
Tube heat capacity (J/(kg·K))	500
Tube density (kg/m^3)	7930
Total number of tubes (−)	6080
Tube bundle layout (−)	Triangular
Tube pitch (m)	0.02
Shell inner diameter (m)	1.571
Shell side maximum flow cross-sectional area (m^2)	0.2468
Number of baffles (−)	12
Baffle thickness (m)	0.02
Baffle cut (%)	25

The axial and circumferential heat conduction of the working fluid and the heat transfer tubes ignored, there is only radial heat conduction;
The radial thermal conductivity of the heat transfer tubes is infinite, namely there is no temperature difference between the inner tube wall and outer tube wall;
The heat loss of oil/salt heat exchanger is ignored;
The arithmetic mean temperature of the working fluid inlet and outlet temperature is used as reference temperature and the lumped parameter temperature.

The model of oil/salt heat exchanger is built based on energy conservation law for open systems. The equations are listed below:
The energy conservation equation of oil side:

$$\frac{d\left(c_{p\_oil}m_{oil}T_{oil}\right)}{dt} = q_{m\_oil}\left(h_{oil\_in} - h_{oil\_out}\right) - Q_{oil} \tag{9}$$

where:

$$h_{oil\_in} = \int_{12^\circ C}^{T_{oil\_in}} c_{p\_oil}dT \tag{9a}$$

$$h_{oil\_out} = \int_{12^\circ C}^{T_{oil\_out}} c_{p\_oil}dT \tag{9b}$$

Heat flow rate between oil and heat transfer tube:

$$Q_{oil} = \alpha A_i(T_{oil} - T_{tube}) \tag{10}$$

where:
heat transfer coefficient α is obtained by Gnielinski formula:

$$\alpha = \frac{(f/8)(Re-1000)Pr_f}{1+12.7\sqrt{f/8}\left(Pr_f^{2/3}-1\right)}\left[1+\left(\frac{d_i}{l}\right)^{2/3}\right]\left(\frac{Pr_f}{Pr_w}\right)^{0.01}\frac{\lambda}{d_i} \quad \left(2300 < Re < 10^6, 0.6 < Pr_f < 10^5, 0.05 < \frac{Pr_f}{Pr_w} < 20\right) \tag{10a}$$

The energy conservation equation of molten salt side:

$$\frac{d\left(c_{p\_salt}m_{salt}T_{salt}\right)}{dt} = q_{m\_salt}\left(h_{salt\_in} - h_{salt\_out}\right) + Q_{salt} \tag{11}$$

where:

$$h_{salt\_in} = \int_{270^\circ C}^{T_{salt\_in}} c_{p\_salt}dT \tag{11a}$$

$$h_{salt\_out} = \int_{270^\circ C}^{T_{salt\_out}} c_{p\_salt}dT \tag{11b}$$

Heat flow rate between molten salt and heat transfer tube:

$$Q_{salt} = \alpha' A_o(T_{tube} - T_{salt}) \tag{12}$$

where:
heat transfer coefficient α' is obtained by Zhukauskas correlations:

$$\alpha' = 1.04Re_f^{0.4}Pr_f^{0.36}\left(\frac{Pr_f}{Pr_w}\right)^{0.25}\frac{\lambda}{d_o} \quad \left(1 \le Re \le 5\times 10^2\right) \tag{12a}$$

$$\alpha' = 0.71Re_f^{0.5}Pr_f^{0.36}\left(\frac{Pr_f}{Pr_w}\right)^{0.25}\frac{\lambda}{d_o} \quad \left(5\times 10^2 < Re \le 10^3\right) \tag{12b}$$

$$\alpha' = 0.35\left(\frac{s_1}{s_2}\right)^{0.2}Re_f^{0.6}Pr_f^{0.36}\left(\frac{Pr_f}{Pr_w}\right)^{0.25}\frac{\lambda}{d_o} \quad \left(10^3 < Re \le 2\times 10^5\right) \tag{12c}$$

$$\alpha' = 0.031\left(\frac{s_1}{s_2}\right)^{0.2}Re_f^{0.8}Pr_f^{0.36}\left(\frac{Pr_f}{Pr_w}\right)^{0.25}\frac{\lambda}{d_o} \quad \left(2\times 10^5 < Re \le 2\times 10^6\right) \tag{12d}$$

The energy conservation equation of heat transfer tube wall:

$$\frac{d\left(c_{p\_tube}m_{tube}T_{tube}\right)}{dt} = Q_{oil} - Q_{salt} \tag{13}$$

2.3. The model of molten salt tank

The model of molten salt tank is built based on energy conservation law for open systems. The heat loss of tank is considered. The equations are listed below:

$$\frac{\partial(u(t)m(t))}{\partial t} = h_{salt\_in}q_{m\_salt} - \alpha_{tank}A_{tank}(T(t) - T_{amb}) \tag{14}$$

where:

$$u(t) = c_{p\_salt}\left(T(t) - T_{ref}\right) \tag{14a}$$

$$m(t) = m_0 + q_{m\_salt}t \tag{14b}$$

$$h_{salt\_in} = c_{p\_salt\_out}\left(T_{salt\_out} - T_{ref}\right) \tag{14c}$$

$\alpha_{tank} = 0.4$, $A_{tank} = 804.25\ m^2$, $T_{amb} = 20\ ^\circ C$, T_{ref} cancels out when

the differential equation is solved by implicit Euler method.

Molten salt height in the tank:

$$H_{salt} = \frac{m(t)}{\rho_{salt}\pi R^2} \tag{15}$$

2.4. The formation of dynamic system model on the STAR-90 simulation platform

The dynamic model of two-tank indirect thermal energy storage system with molten salt is built on the STAR-90 simulation platform for real-time simulation. The mathematical model built above is differential form, which cannot be applied on the simulation platform, so it is necessary to convert differential equations into the form which the simulation platform can identify. Therefore, the differential equations are converted into the difference equations and the implicit Euler method is used. For example, equation (9) can be converted into:

$$T_{oil\_out} = T^0_{oil\_out} + \frac{q_{m\_oil}\left(h_{oil\_in} - h^0_{oil\_out}\right) - \alpha A_i\left(T^0_{oil} - T^0_{tube}\right)}{c^0_{p\_oil}m^0_{oil}/(2\Delta t) + \alpha A_i/2} \tag{16}$$

3. System dynamic simulations

3.1. Dynamic simulation of charging process

The dynamic simulation of charging process is described as follows: heat transfer oil inlet temperature (393 °C) in oil/salt heat exchanger, molten salt temperature (292 °C) in the cold salt tank and heat transfer oil flow rate (568.3 kg/s) and molten salt flow rate (931.3 kg/s) remain constant. The initial heat transfer oil outlet temperature, the initial molten salt outlet temperature in oil/salt heat exchanger and the initial heat transfer tube wall temperature is set for 12 °C, 292 °C, 270 °C respectively. The radius of the salt tank is 8 m and the height is 12 m. The initial molten salt temperature, the initial molten salt height and the initial molten salt mass in the hot salt tank is 300 °C, 0.5 m, 190811.52 kg respectively. The initial molten salt height in the cold salt tank is 10 m and the molten salt mass pumped from the cold tank is 4209569.41 kg. The dynamic simulation of charging process is started by opening heat transfer oil pump, cold salt tank pump and hot salt tank valve. The simulation results are shown as Fig. 2:

3.2. Dynamic simulation of discharging process

The dynamic simulation of discharging process is described as follows: heat transfer oil inlet temperature (299 °C) in oil/salt heat exchanger, molten salt temperature (386 °C) in the hot salt tank and heat transfer oil flow rate (568.3 kg/s) and molten salt flow rate (931.3 kg/s) remain constant. The initial heat transfer oil outlet temperature, the initial molten salt outlet temperature in oil/salt heat exchanger and the initial heat transfer tube wall temperature is set for 299 °C, 386 °C, 270 °C respectively. The radius of the salt tank is 8 m and the height is 12 m. The initial molten salt temperature, the initial molten salt height and the initial molten salt mass in the cold salt tank is 292 °C, 0.5 m, 191344.064 kg respectively. The initial molten salt height in the hot salt tank is 10 m and the molten salt mass pumped from the hot tank is 4209569.41 kg. The dynamic simulation of discharging process is started by opening heat transfer oil pump, hot salt tank pump and cold salt tank valve. The simulation results are shown as Fig. 3:

3.3. Dynamic simulation of heat transfer oil flow rate disturbance in the charging process

Due to the instability of solar irradiation, heat transfer oil flow rate usually varies in order to ensure the stability of heat transfer oil outlet temperature in the solar field. Therefore, the variation of heat transfer oil flow rate is considered in the charging process. When flow rate disturbance is simulated, the molten salt flow rate (931.3 kg/s) remains constant and heat transfer oil flow rate steps down from 568.3 kg/s to 300 kg/s. Then when remains 300 kg/s for 120s, heat transfer oil flow rate steps up to 568.3 kg/s again and lasts for 270s. Then heat transfer oil flow rate steps up from 568.3 kg/s to 800 kg/s. Eventually when remains 800 kg/s for 120s, heat transfer oil flow rate returns to the rated flow rate 568.3 kg/s. The simulation results are shown as Fig. 4:

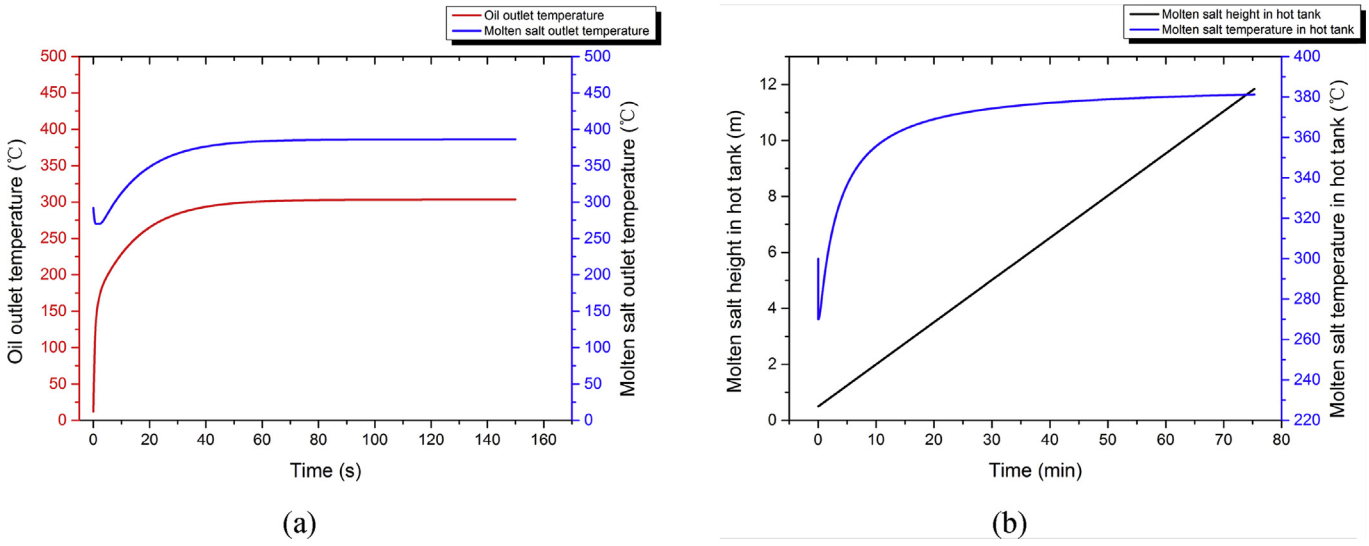

Fig. 2. The dynamic simulation results of charging process.

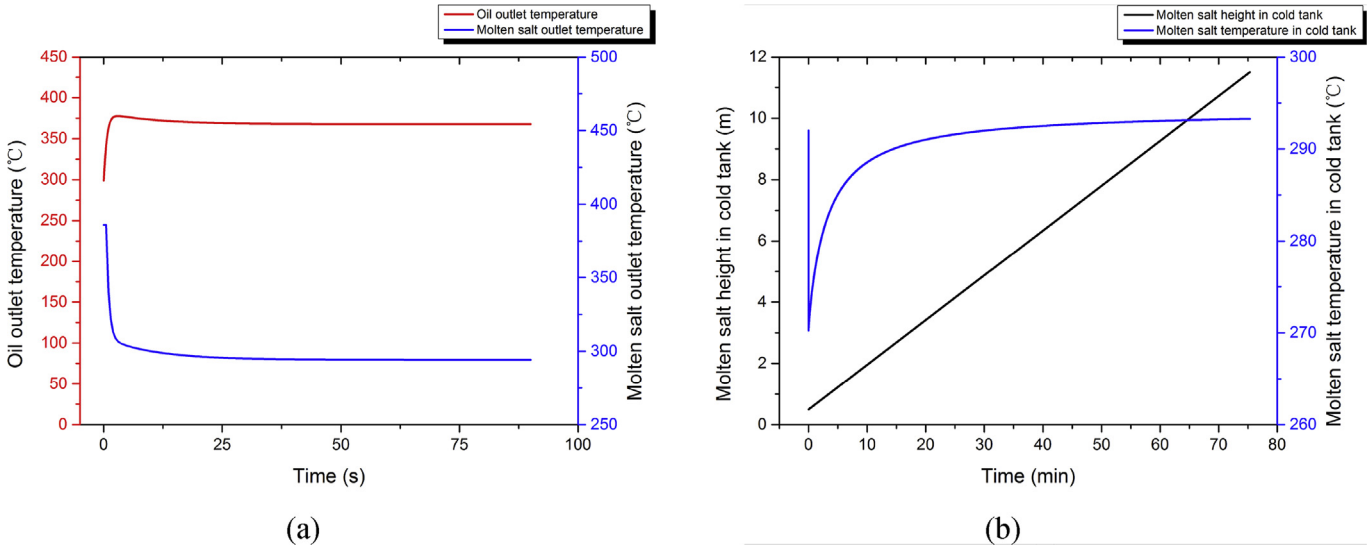

Fig. 3. The dynamic simulation results of discharging process.

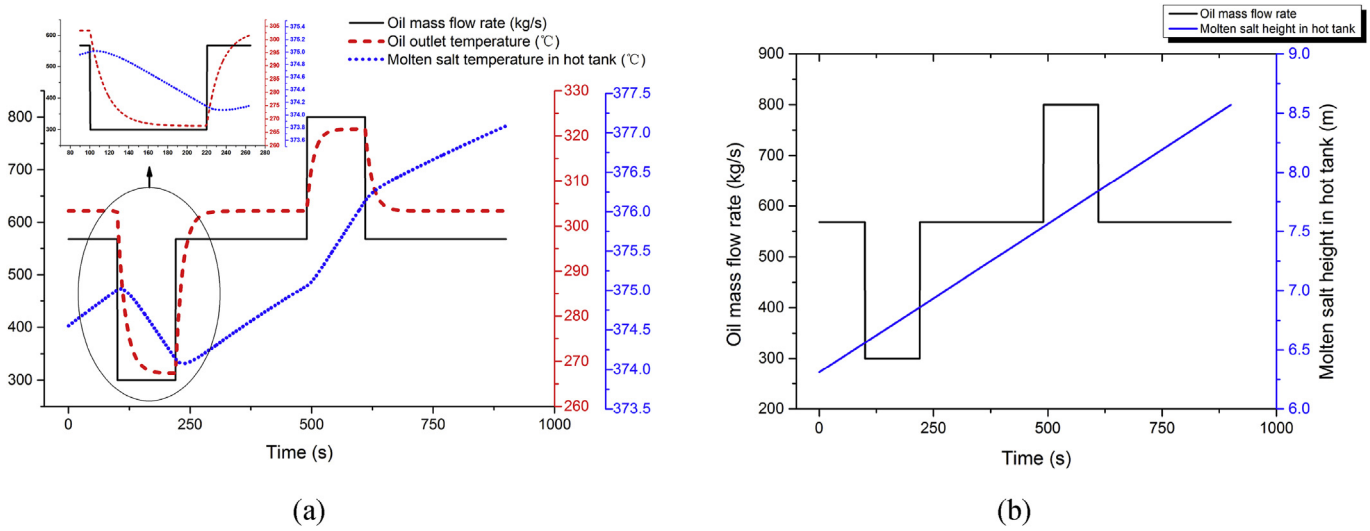

Fig. 4. The dynamic simulation results of heat transfer oil flow rate disturbance in the charging process.

3.4. Dynamic simulation of heat transfer oil flow rate disturbance in the discharging process

The heat transfer oil flow rate varies with the steam flow rate because steam turbine often runs under varying duty condition and steam turbine varying duty operation can be achieved by adjusting the steam flow rate and keeping the steam parameters before steam turbine constant. Therefore, although the molten salt is heat source in the discharging process, it is more meaningful to study the influence of heat transfer oil flow rate disturbance on the discharging process. When flow rate disturbance is simulated, the molten salt flow rate (931.3 kg/s) remains constant and heat transfer oil flow rate steps down from 568.3 kg/s to 300 kg/s. Then when remains 300 kg/s for 120s, heat transfer oil flow rate steps up to 568.3 kg/s again and lasts for 270s. Then heat transfer oil flow rate steps up from 568.3 kg/s to 800 kg/s. Eventually when remains 800 kg/s for 120s, heat transfer oil flow rate returns to the rated flow rate 568.3 kg/s. The simulation results are shown as Fig. 5:

4. Discussions

As the simulation results of charging process and discharging process indicate, the time that heat transfer oil outlet temperature and molten salt outlet temperature in oil/salt heat exchanger reach to stability is short. The time is about 40s for charging process and 50s for discharging process. The molten salt temperature in the salt tank both decreases rapidly at first and then gradually increases in the charging and discharging processes, but the reasons are different. For charging process, since the initial molten salt outlet temperature in oil/salt heat exchanger is set lower than the molten salt temperature in hot salt tank, the molten salt temperature in hot salt tank drops rapidly at the beginning of charging process. As the charging process continues, the molten salt outlet temperature in oil/salt heat exchanger gradually increases. The molten salt temperature in hot salt tank will increase when the molten salt outlet temperature in oil/salt heat exchanger rises above the molten salt temperature in hot salt tank; For discharging process, although the

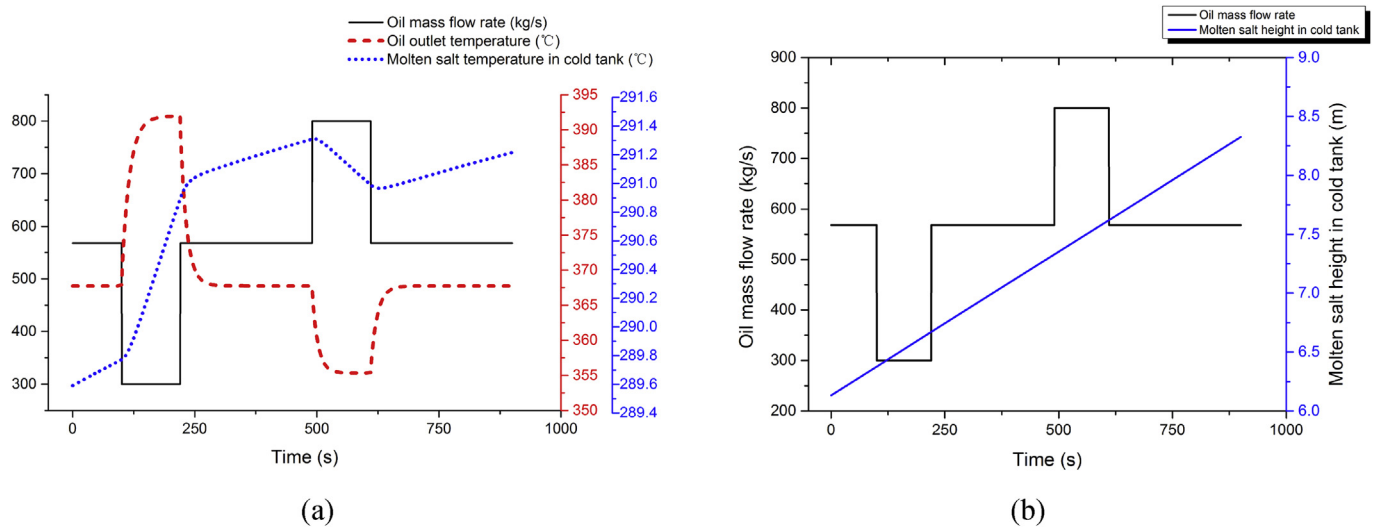

Fig. 5. The dynamic simulation results of heat transfer oil flow rate disturbance in the discharging process.

initial molten salt outlet temperature in oil/salt heat exchanger is set higher than the molten salt temperature in cold salt tank, the molten salt temperature in cold salt tank still drops rapidly at the beginning of discharging process. The reason is that the heat loss of cold salt tank is greater than the energy of the molten salt into cold salt tank. The molten salt temperature in the cold salt tank begins to increase gradually when the energy of the molten salt into cold salt tank is greater than the heat loss of cold salt tank. As is also be seen from the simulation results, although the variation of molten salt physical properties with temperature is considered, the change of molten salt height in the tank is still approximately linear. The duration of the charging and discharging processes is 75.3min.

In the simulation of heat transfer oil flow rate disturbance, the data is recorded when the time reaches 38.6min and lasts 15min (900s), and the disturbance starts at 40.3min. As can be seen, when heat transfer oil flow rate steps up and steps down, the changes of heat transfer oil outlet temperature in oil/salt heat exchanger are opposite in both charging process and discharging process. It can also be seen from the simulation results, when step change of heat transfer oil flow rate happens, heat transfer oil outlet temperature gradually reaches a new stable value, which can be called thermal inertia.

In addition, in the charging process, as is shown in the small figure of Fig. 4, when heat transfer oil flow rate steps down, heat transfer oil outlet temperature instantly begins to decrease, while the molten salt temperature in hot salt tank begins to decrease after continuing to increase for a short time; when heat transfer oil flow rate returns to the rated value, heat transfer oil outlet temperature instantly begins to increase, while the molten salt temperature in hot salt tank begins to increase after continuing to decrease for a short time. The reason is that when heat transfer oil flow rate steps down, the molten salt outlet temperature in oil/salt heat exchanger will decrease, but it is still higher than the molten salt temperature in hot salt tank at the early time, therefore the molten salt temperature in hot salt tank still increases until the molten salt outlet temperature in oil/salt heat exchanger is lower than the molten salt temperature in hot salt tank; when heat transfer oil flow rate returns to the rated value, the molten salt outlet temperature in oil/salt heat exchanger will increase, but it is still lower than the molten salt temperature in hot salt tank at the early time, therefore the molten salt temperature in hot salt tank still decreases until the molten salt outlet temperature in oil/salt heat exchanger is higher than the molten salt temperature in hot salt tank. When heat transfer oil flow rate steps up, heat transfer oil outlet temperature instantly begins to increase. Meanwhile, the molten salt temperature in hot salt tank also begins to increase instantly, and the change rate is greater than that before; when heat transfer oil flow rate returns to the rated value, the change rate returns to the normal. In the process, the molten salt temperature in hot salt tank always increases. In the discharging process, the relationship between the variation of heat transfer oil outlet temperature and the molten salt temperature in cold salt tank is the same as that in the charging process.

As can also be seen from Figs. 4 and 5, although the molten salt temperature in molten salt tanks changes due to heat transfer oil flow rate disturbance, which leads to variation of molten salt physical properties, the change of molten salt height in the tank is still approximately linear.

5. Conclusions

In this passage, a universal dynamic simulation model of two-tank indirect thermal energy storage system with molten salt based on the lumped parameter method is built. The obtained conclusions are as follows:

In the charging and discharging processes, the time heat transfer oil outlet temperature and molten salt outlet temperature in oil/salt heat exchanger reach to the stable value is very short, about 40–50s;

In the dynamic simulation of heat transfer oil flow rate disturbance, when heat transfer oil outlet temperature in oil/salt heat exchanger firstly decreases and then returns to the rated value, the change of molten salt temperature in molten salt tanks is the same as heat transfer oil outlet temperature, but always lags behind it; when heat transfer oil outlet temperature in oil/salt heat exchanger firstly increases and then returns to the rated value, molten salt temperature in molten salt tanks always increases, but the change rate will vary;

In the charging and discharging processes, although the variation of molten salt physical properties with temperature is considered, the change of molten salt height in the tank is still approximately linear.

Acknowledgements

This work has been supported by National High Technology Research and Development Program (863 Program): trough collectors, power generation systems experimental platform research and demonstration (2012AA050603), National Natural Science Foundation of China (51476164), Science and Technology Project of China State Grid Corporation (NY71-15-040).

References

[1] F. Dinter, D. Mayorga Gonzalez, Operability, reliability and economic benefits of CSP with thermal energy storage: first year of operation of ANDASOL 3, Energy Procedia 49 (2014) 2472–2481.
[2] Ulf Herrmann, Bruce Kelly, Henry Price, Two-tank molten salt storage for parabolic trough solar power plants, Energy 29 (2004) 883–893.
[3] Jie Yang, Lei Ma, Jessica Bock, Anthony M. Jacobi, Wei Liu, A comparison of four numerical modeling approaches for enhanced shell-and-tube heat exchangers with experimental validation, Appl. Therm. Eng. 65 (2014) 369–383.
[4] C.K. Lee, A modified three-dimensional numerical model for predicting the short-time-step performance of borehole ground heat exchangers, Renew. Energy 87 (2016) 618–627.
[5] Gabriel Batalha Leoni, Tânia Suaiden Klein, Ricardo de Andrade Medronho, Assessment with computational fluid dynamics of the effects of baffle clearances on the shell side flow in a shell and tube heat exchanger, Appl. Therm. Eng. 112 (2017) 497–506.
[6] Fabio De Bellis, Luciano A. Catalano, CFD optimization of an immersed particle heat exchanger, Appl. Energy 97 (2012) 841–848.
[7] Aniket Shrikant Ambekar, R. Sivakumar, N. Anantharaman, M. Vivekenandan, CFD simulation study of shell and tube heat exchangers with different baffle segment configurations, Appl. Therm. Eng. 108 (2016) 999–1007.
[8] Mahmoud Galal Yehia, Ahmed A.A. Attia, Osama Ezzat Abdelatif, Essam E. Khalil, Heat transfer and friction characteristics of shell and tube heat exchanger with multi inserted swirl vanes, Appl. Therm. Eng. 102 (2016) 1481–1491.
[9] Jie Yang, Wei Liu, Numerical investigation on a novel shell-and-tube heat exchanger with plate baffles and experimental validation, Energy Convers. Manag. 101 (2015) 689–696.
[10] Fritz Zaversky, Marcelino Sánchez, David Astrain, Object-oriented modeling for the transient response simulation of multi-pass shell-and-tube heat exchangers as applied in active indirect thermal energy storage systems for concentrated solar power, Energy 65 (2014) 647–664.
[11] Ismael Rodríguez Maestre, Francisco Javier González Gallero, Pascual Álvarez Gómez, Luis Pérez-Lombard, A new RC and g-function hybrid model to simulate vertical ground heat exchangers, Renew. Energy 78 (2015) 631–642.
[12] Simon J. Rees, An extended two-dimensional borehole heat exchanger model for simulation of short and medium timescale thermal response, Renew. Energy 83 (2015) 518–526.
[13] Ka-Kui Tse, Tin-Tai Chow, Dynamic model and experimental validation of an indirect thermosyphon solar water heater coupled with a parallel circular tube rings type heat exchange coil, Sol. Energy 114 (2015) 114–133.
[14] Flavio Manenti, Zohreh Ravaghi-Ardebil, Dynamic simulation of concentrating solar power plant and two-tanks direct thermal energy storage, Energy 55 (2013) 89–97.
[15] Javier Bonilla, Margarita M. Rodríguez-García, Lidia Roca, Loreto Valenzuela, Object-oriented modeling of a multi-pass shell-and-tube heat exchanger and its application to performance evaluation, IFAC-PapersOnLine 48–11 (2015) 097–102.
[16] Solutia, Therminol VP-1 heat transfer fluid-Vapour and Liquid phases, Tech. Bull. (2008) 3, 7239115C.
[17] A.B. Zavoico, Solar Power Tower - Design Basis Document. Technical Report SAND2001-2100, Sandia National Laboratories, Albuquerque, USA, 2001.